In vivo selective inhibition of TRPC6 by antagonist BI 749327 ameliorates fibrosis and dysfunction in cardiac and renal disease

Brian Leei Lin[a], Damian Matera[b], Julia F. Doerner[c], Nan Zheng[c], Donato del Camino[c], Sumita Mishra[a], Hong Bian[b], Svetlana Zeveleva[b], Xiaoguang Zhen[c], Nathaniel T. Blair[c], Jayhong A. Chong[c], David P. Hessler[c], Djahida Bedja[a], Guangshuo Zhu[a], Grace K. Muller[a], Mark J. Ranek[a], Lynn Pantages[b], Mary McFarland[b], Matthew R. Netherton[d], Angela Berry[d], Diane Wong[d], Georg Rast[e], Hu Sheng Qian[b], Steven M. Weldon[b], Jay J. Kuo[b], Achim Sauer[e], Chris Sarko[d], Magdalene M. Moran[c], David A. Kass[a,1], and Steven S. Pullen[b,1]

[a]Division of Cardiology, Johns Hopkins Medical Institutions, Baltimore, MD 21205; [b]Cardiometabolic Diseases Research, Boehringer Ingelheim Pharmaceuticals, Inc., Ridgefield, CT 06877; [c]Hydra Biosciences, Cambridge, MA 02138; [d]Small Molecule Discovery Research, Boehringer Ingelheim Pharmaceuticals, Inc., Ridgefield, CT 06877; and [e]Drug Discovery Sciences, Boehringer Ingelheim GmbH & Co. KG, 88397 Biberach an der Riss, Germany

Edited by Christine E. Seidman, Howard Hughes Medical Institute, Brigham and Women's Hospital, and Harvard Medical School, Boston, MA, and approved March 28, 2019 (received for review September 7, 2018)

Transient receptor potential canonical type 6 (TRPC6) is a nonselective receptor-operated cation channel that regulates reactive fibrosis and growth signaling. Increased TRPC6 activity from enhanced gene expression or gain-of-function mutations contribute to cardiac and/or renal disease. Despite evidence supporting a pathophysiological role, no orally bioavailable selective TRPC6 inhibitor has yet been developed and tested in vivo in disease models. Here, we report an orally bioavailable TRPC6 antagonist (BI 749327; IC_{50} 13 nM against mouse TRPC6, $t_{1/2}$ 8.5–13.5 hours) with 85- and 42-fold selectivity over the most closely related channels, TRPC3 and TRPC7. TRPC6 calcium conductance results in the stimulation of nuclear factor of activated T cells (NFAT) that triggers pathological cardiac and renal fibrosis and disease. BI 749327 suppresses NFAT activation in HEK293T cells expressing wild-type or gain-of-function TRPC6 mutants (P112Q, M132T, R175Q, R895C, and R895L) and blocks associated signaling and expression of prohypertrophic genes in isolated myocytes. In vivo, BI 749327 (30 mg/kg/day, yielding unbound trough plasma concentration ∼180 nM) improves left heart function, reduces volume/mass ratio, and blunts expression of profibrotic genes and interstitial fibrosis in mice subjected to sustained pressure overload. Additionally, BI 749327 dose dependently reduces renal fibrosis and associated gene expression in mice with unilateral ureteral obstruction. These results provide in vivo evidence of therapeutic efficacy for a selective pharmacological TRPC6 inhibitor with oral bioavailability and suitable pharmacokinetics to ameliorate cardiac and renal stress-induced disease with fibrosis.

TRPC6 | ion channels | calcium | nuclear factor of activated T cells | fibrosis

The transient receptor potential canonical 6 (TRPC6) channel is a nonselective cation channel expressed in multiple cell types. TRPC6 plays physiological roles as a regulator of smooth muscle contraction, pulmonary endothelial permeability, slit-diaphragm structure and function of renal podocytes, and neuronal protection against ischemia (1). However, TRPC6 hyperactivity contributes to disease, including that of the systemic and pulmonary circulations (2), cardiac myocytes (3), and renal podocytes (4). Human TRPC6 gain-of-function mutations cause familial focal segmental glomerulosclerosis (4–8), while TRPC6 up-regulation in the heart as observed with abnormal hemodynamic stress stimulates pathological muscle growth and dysfunction (1, 3, 9–11). TRPC6 up-regulation also contributes to hypoxic vasoconstriction associated with pulmonary edema (2, 12, 13). TRPC6 cation conductance is linked to calcium activation of the phosphatase calcineurin (Cn) that in turn stimulates nuclear factor of activated T cells (NFAT) transcriptional regulation (14–17). NFAT enhances TRPC6 gene expression itself, forming a positive feedback loop. TRPC6 expression is also enhanced by transforming growth factor-beta and other profibrotic factors via p38-dependent stimulation of serum response factor, to activate myofibroblasts (18).

To date, the role of TRPC6 signaling has been mostly studied using genetic gain- or loss-of-function mouse models. Transgenic TRPC6 overexpression of wild-type (WT) or gain-of-function mutants in podocytes leads to hyperalbuminuria (19), and WT-TRPC6 overexpression in cardiac myocytes induces hypertrophy, fibrosis, and heart failure (9). Unilateral ureteral obstruction (UUO)-induced renal injury in mice increases TRPC6 gene expression and results in marked interstitial fibrosis that is blunted

Significance

Transient receptor potential canonical 6 (TRPC6) is an important mediator of pathological hypertrophy and fibrosis, contributing to renal and cardiac disease. However, no selective TRPC6 inhibitor with in vivo efficacy has been developed and tested to determine if nongenetic channel suppression ameliorates disease in intact animals. We developed and tested an orally bioavailable TRPC6-specific inhibitor, BI 749327, revealing its capacity to improve cardiac function and reduce chamber dilation and fibrosis in the context of abnormal hemodynamic stress. Similarly, BI 749327 suppressed myofibroblast activation and fibrosis in a renal disease model. These data support BI 749327 as a representative of a therapeutic class for treating cardiac and renal disease and provide a tool for studying the biological function of TRPC6.

Author contributions: B.L.L., D.M., J.F.D., D.d.C., D.W., J.J.K., A.S., C.S., M.M.M., D.A.K., and S.S.P. designed research; B.L.L., D.M., J.F.D., N.Z., D.d.C., S.M., H.B., S.Z., X.Z., N.T.B., J.A.C., D.P.H., D.B., G.Z., G.K.M., L.P., and M.M. performed research; M.R.N., A.B., and C.S. contributed new reagents/analytic tools; B.L.L., D.M., J.F.D., N.Z., D.d.C., S.M., H.B., S.Z., X.Z., N.T.B., J.A.C., D.P.H., D.B., G.K.M., M.J.R., D.W., G.R., H.S.Q., S.M.W., J.J.K., A.S., M.M.M., D.A.K., and S.S.P. analyzed data; and B.L.L., G.R., A.S., D.A.K., and S.S.P. wrote the paper.

Conflict of interest statement: D.M., J.F.D., L.P., D.W., G.R., S.M.W., S.Z., H.S.Q, J.J.K, A.S., and S.S.P. are full-time employees of Boehringer Ingelheim Pharmaceuticals, Inc. M.M, M.R.N, A.B., and C.S. were full-time employees of Boehringer Ingelheim Pharmaceuticals, Inc. A.B. and M.R.N. are listed as coinventors on a US provisional patent application filed by Boehringer Ingelheim Pharmaceuticals, Inc. relevant to this work. J.F.D., N.Z., D.d.C., X.Z., N.T.B., J.A.C., D.P.H., and M.M.M. were employees of Hydra Biosciences, and received options. This work was supported in part by Boehringer Ingelheim Pharmaceuticals, Inc.

This article is a PNAS Direct Submission.

[1]To whom correspondence may be addressed. Email: dkass@jhmi.edu or steven.pullen@boehringer-ingelheim.com.

This article contains supporting information online at www.pnas.org/lookup/suppl/doi:10.1073/pnas.1815354116/-/DCSupplemental.

Published online April 26, 2019.

in TRPC6-deficient mice (20). TRPC6-knockout (KO) mice also develop less lung fibrosis in bleomycin-treated animals and following lung ischemia/reperfusion injury (2, 21). However, gene deletion in the heart does not suppress pathological hypertrophy or dysfunction induced by pressure stress (3), whereas overexpression of a dominant negative TRPC6 is protective (11). Importantly, all of these genetic models alter TRPC6 expression at an embryonic or neonatal stage, well before the induction of disease. To our knowledge, no prior studies have tested the therapeutic efficacy of selective pharmacological TRPC6 inhibition in a nongenetically modified animal at or after the onset of disease.

A major impediment to translational testing of TRPC6 inhibition has been the lack of a potent, selective, and orally bioavailable inhibitor. Previously reported blockers were nonselective, with comparable potency against TRPC3 and/or TRPC7, the two channels with highest homology to TRPC6. They include: SKF 96365, 2-aminoethoxydiphenyl borate, BTP2, larixol analogs, GSK2332255B, GSK2833503A, norgestimate, 8009-5364, pyrazolo[1,5-a]pyrimidine, and GsMTx-4 (3, 22–30). SAR7334 was recently identified as a TRPC6 antagonist with 30- and 24-fold selectivity against TRPC3 and TRPC7, respectively, but has rapid in vivo clearance (31). An analog, DS88790512, has improved pharmacokinetics, but its selectivity profile and in vivo efficacy remain unreported (32).

The present effort aimed to identify an orally bioavailable, selective, and potent TRPC6 inhibitor to allow testing of the role of TRPC6 in animal models of cardiac and renal disease. Using a high-throughput screen and medicinal chemistry, we identified BI 749327 with nanomolar potency, high selectivity, pharmacokinetic properties compatible with once-daily dosing, and low peak-to-trough plasma exposure ratios. We then tested its efficacy in two relevant disease models: cardiac hypertrophy and fibrosis induced by sustained pressure overload (PO) stress and renal fibrosis induced by UUO. We report therapeutic efficacy of oral TRPC6 suppression in both models, supporting its utility to treat heart and renal disease and potentially other disorders impacted by excessive TRPC6 ion channel activity.

Results

Identification and in Vitro Profile of BI 749327. We performed a high-throughput screen using HEK293 cells stably transfected to express human TRPC6 and stimulated with 1-oleoyl-2-acetyl-sn-glycerol (OAG) to identify TRPC6 antagonists using a fluorescent readout for membrane potential. Medicinal chemistry, aimed to optimize compound potency, selectivity against related (TRPC3/5/7) and unrelated (Kv11.1) ion channels, and subsequent pharmacokinetics, yielded BI 749327 (Fig. 1*A*). Using whole-cell patch clamp in a heterologous expression system, HEK293 cells made to express TRPC6, we find BI 749327 potently inhibits OAG-activated mouse TRPC6 current with an IC_{50} of 13 nM (Fig. 1*B* and *SI Appendix*, Table S1). BI 749327 has similar potency against human (IC_{50} = 19 nM) and guinea pig (IC_{50} = 15 nM) TRPC6. TRPC3 and TRPC7 are the most homologous to TRPC6, sharing similar activation mechanisms, and BI 749327 is 85-fold more selective for mouse TRPC6 than TRPC3 (IC_{50} = 1,100 nM) and 42-fold versus TRPC7 (IC_{50} = 550 nM, Fig. 1*C*), and minimally inhibits TRPC5 (>700-fold selective, *SI Appendix*, Table S1), another channel proposed to play a role in renal function (4, 33). BI 749327 had >500-fold TRPC6 selectivity versus human TRPM8, TRPV1, TRPA1, and Nav1.5 and >150-fold selectivity against human Kv11.1 (hERG) (*SI Appendix*, Table S2).

BI 749327 Blocks Hypertrophic Signaling in Cells Expressing WT or Mutant TRPC6. To test the impact of BI 749327 on TRPC6-related molecular signaling, HEK293T cells were transfected with an NFAT-luciferase reporter and plasmids expressing either TRPC6 or empty vector (Fig. 2*A*). NFAT luciferase activity increased with forced TRPC6 expression and was dose-dependently inhibited by BI 749327, with the highest dose (500 nM) abrogating activation. The same high dose (500 nM) had no impact on NFAT activity in cells transfected with empty vector or with TRPC3, though mild inhibition of TRPC7-mediated NFAT promoter activation was observed, consistent with IC_{50} data (*SI Appendix*, Fig. S1*A*). BI 749327 also reduced NFAT activation in HEK293T cells expressing gain-of-function TRPC6 mutants that cause familial glomerulosclerosis in humans (P112Q, M132T, R175Q, R895C, and R895L) (4–8). The first three mutations reside in the N terminus and the latter in the C terminus, and their induction of NFAT activity was fully blocked by 500 nM BI 749327 (Fig. 2*B*).

TRPC6 is required for angiotensin II (Ang II)-induced hypertrophic signaling in cardiomyocytes (34). We therefore tested whether BI 749327 modifies hypertrophic gene regulation in neonatal rat ventricular myocytes exposed to Ang II (100 μM for 48 h). Ang II stimulated mRNA expression of genes coupled to pathological hypertrophy (*Nppa*, *Nppb*, and *Myh7*) and to Cn/NFAT signaling (*Rcan1* and *Trpc6*) (Fig. 2*C*). This increase was attenuated by exposure to 250 or 500 nM BI 749327. BI 749327 did not alter the expression of these hypertrophic gene markers in the absence of Ang II (*SI Appendix*, Fig. S1*B*).

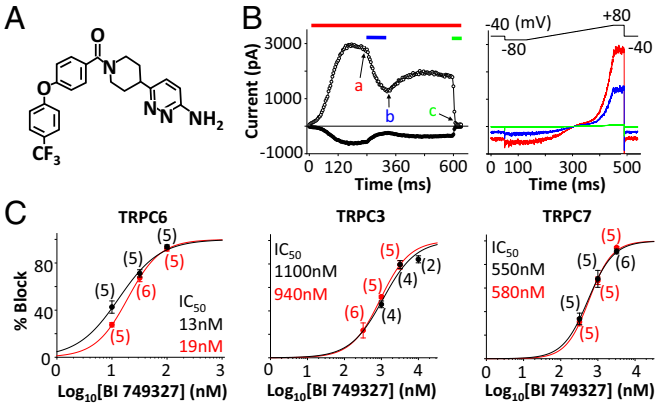

Fig. 1. BI 749327 inhibition of recombinantly expressed TRPC channels. (*A*) Structure of BI 749327. (*B*, *Left*) Inward (filled circles, −80 mV) and outward (open circles, +80 mV) mTRPC6 currents activated in the presence of 1 μM OAG (red bar), during exposure to 10 nM (blue bar) and 1 μM (green bar) BI 749327. (*B*, *Right*) mTRPC6 current–voltage relations taken at time points indicated in *B*, *Left*: a, 1 μM OAG (red trace); b, 10 nM BI 749327 (blue trace); and c, 1 μM BI 749327 (green trace). (*C*) Concentration–response curves of TRPC6, TRPC3, and TRPC7 channel inhibition by BI 749327 with calculated IC_{50} (mouse, black; human, red). Symbols represent the average percent inhibition recorded for the indicated number of cells per concentration. Solid lines are logistic fits to the averages measured at three concentrations.

Pharmacokinetic Profiling. To test the efficacy of BI 749327 in vivo, we first performed single dose pharmacokinetic (PK) experiments to guide the studies. Oral administration of 3, 10, or 30 mg/kg BI 749327 to CD-1 mice led to a dose-proportional increase of maximum plasma concentrations (C_{max}) and total systemic exposure (*SI Appendix*, Fig. S2*A* and Table S3). The long terminal half-life ($t_{1/2}$) of 8.5–13.5 h qualified the compound for once daily oral dosing. Oral administration of 30 mg/kg BI 749327 to B6129F1, CD-1, and C57BL/6J mice yielded comparable exposures (*SI Appendix*, Fig. S2). These datasets were then used to develop a two compartment PK model to simulate multiple dosing. Mouse plasma protein binding of BI 749327 measured by equilibrium dialysis was high at 98.4 ± 0.1% (at a concentration of 1 μM) with a corresponding unbound fraction of 1.6%. Given this, the trough unbound concentration was ~180 nM using daily 30 mg/kg oral dosing, 10× the IC_{50} for TRPC6, and 1/5–1/6 the IC_{50} for TRPC7 and TRPC3.

PHYSIOLOGY

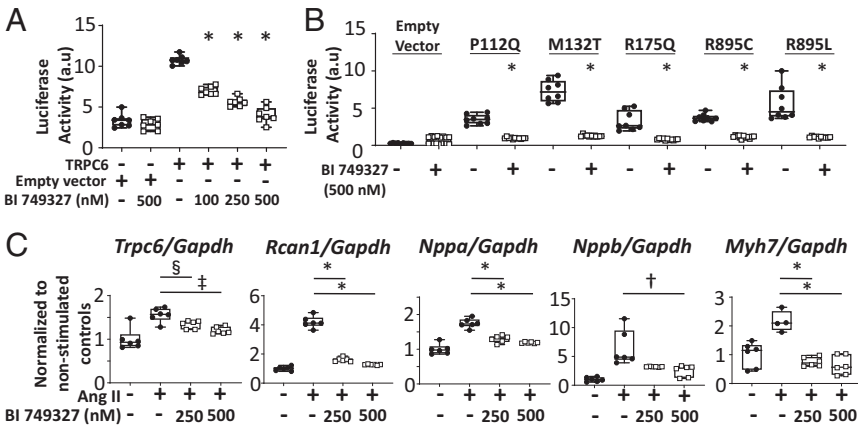

Fig. 2. Efficacy of BI 749327 on TRPC6-mediated signaling in vitro. (*A*) NFAT activity in HEK293T cells mediated by TRPC6 expression is blunted by BI 749327 in a dose-dependent manner (*$P < 0.0001$, $n = 6$ per group, one-way ANOVA, Tukey pairwise comparison). (*B*) NFAT activity in HEK293T cells mediated by known TRPC6 gain-of-function mutations (P112Q, M132T, R175Q, R895C, and R895L) is blocked by BI 749327 (500 nM) (*$P < 0.0001$, $n \geq 6$ per group, Mann–Whitney test). (*C*) Ang II-mediated increase in prohypertrophic signaling genes is blocked by BI 749327. Expression of *Trpc6*, *Rcan1*, *Nppa*, *Nppb*, and *Myh7*, normalized to *Gapdh*, is shown. One-way ANOVA with Holm–Sidak pairwise comparisons test, or Kruskal–Wallis with Dunn's test, $n \geq 6$ per group. *$P < 0.0001$; †$P = 0.0014$; ‡$P = 0.0018$; §$P = 0.028$.

Effects of Chronic Oral BI 749327 on Heart Response to Pressure Overload. To test the efficacy of BI 749327 against cardiac disease in vivo, C57BL/6J mice were subjected to transaortic constriction (TAC) surgery to induce pressure overload or to sham surgery. All mice received vehicle gavage 1 wk before TAC to acclimate them to the procedure. Baseline and 1-wk post-TAC echocardiograms were obtained, and mice were then randomized to receive vehicle or 30 mg/kg/d BI 749327 by oral gavage. Mice with post-TAC fractional shortening (FS) above 20% but less than 40% before drug randomization provided the primary study group. Total plasma peak and trough exposure to BI 749327 was similar between drug-treated sham and TAC groups (*SI Appendix*, Fig. S3), and this daily dose did not alter mean arterial pressure or heart rate in conscious mice (*SI Appendix*, Fig. S4). TAC depressed FS was similar in both treatment arms before randomization. Thereafter, BI 749327 led to a gradual increase in FS over vehicle (Fig. 3*A*, **$P = 0.007$ by ANCOVA). Heart end-diastolic and end-systolic dimensions with drug treatment trended to decline, with $P = 0.055$ for end-systolic dimension (*SI Appendix*, Fig. S5 *A* and *B*). BI 749327 did not suppress cardiac hypertrophy (Fig. 3 *B* and *C* and *SI Appendix*, Fig. S5*C*), though the geometry of the heart changed with a greater wall thickness/dimension ratio (cardiac geometry index), reflecting more concentric hypertrophy (Fig. 3*D*, $P = 0.02$ by ANCOVA).

More direct analysis of left ventricular (LV) function was provided by invasive pressure–volume (PV) analysis ($n = 5$–6 per group). Representative PV loops are shown in Fig. 4*A* and summary results in the remaining panels. LV end-diastolic and end-systolic volumes generally significantly declined with BI 749327 treatment, in both sham and TAC groups (Fig. 4*B*). This was associated with a lower stroke volume in the TAC group (Fig. 4*C*). There were no changes in heart rate or other morphometric parameters (Fig. 4*D* and *SI Appendix*, Fig. S5 *D*–*F*). Systolic pressure rose equally with TAC in both groups, and BI 749327 did not change systolic pressure (Fig. 4*E*). Contractility was assessed by load-independent measures [preload-recruitable stroke work (PRSW) and end-systolic elastance (Ees)], and neither was altered by BI 749327 with or without TAC (Fig. 4*F*). Relaxation rate was prolonged by TAC ($P = 0.003$ by two-way ANOVA) but unaltered by active treatment (Fig. 4*G*). Together, these results reveal a reduction in chamber volumes that cannot be ascribed to greater contractility or reduced vascular resistance, but are more compatible with lower cardiac preload from either venodilation or less circulatory volume.

BI 749327 Reduces Pathological Growth and Fibrotic Gene Expression. Similar to that observed in vitro, BI 749327 reduced TAC-induced expression of fetal genes, *Nppa* and *Nppb*, both biomarkers of pathological hypertrophy (Fig. 5*A*). TRPC6 expression declined and *Rcan1* trended downward, supporting interruption of the feedback loop whereby TRPC6 current activates NFAT to in turn up-regulate *Trpc6* gene expression (9). Gene expression of *Trpc1* and *Trpc3*, two channels also linked with TAC-induced cardiac disease, were unaltered by BI 749327 (*SI Appendix*, Fig. S6). TAC increased genes associated with reactive fibrosis, including collagen 1a and 3a (*Col1a2* and *Col3a2*), fibronectin (*Fn1*), metalloproteinase 2 (*Mmp2*), transforming

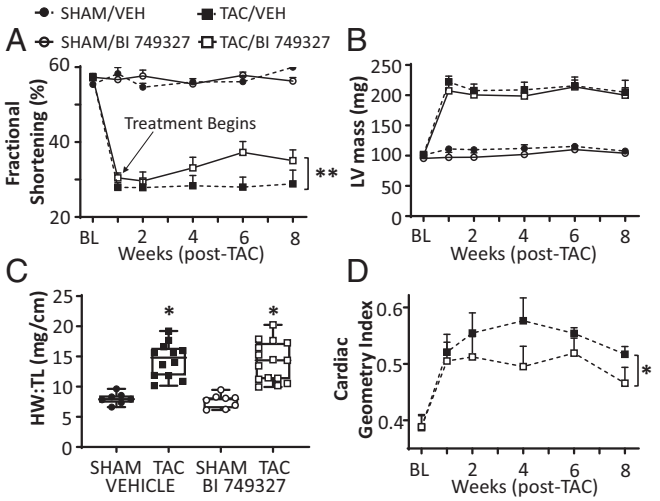

Fig. 3. LV function and morphology in mice treated with vehicle or BI 749327. (*A*) Time course of cardiac function assessed by fractional shortening (%FS) in vehicle- versus BI 749327-treated cohorts. Treatment is randomized after week 1. (**$P = 0.007$, ANCOVA). (*B*) Echocardiographic measurement of LV mass increased by TAC in two study groups ($P < 0.0001$ for effect of TAC; one-way ANOVA). BI 749327 treatment had no impact ($P = 0.99$ between TAC groups). (*C*) Heart weight/tibia length (HW/TL) ratio increases similarly after TAC in both vehicle- and drug-treated groups ($P < 0.0001$ for TAC effect, $P = 0.7$ for drug effect, and $P = 0.92$ for drug × TAC interaction; two-way ANOVA). (*D*) Cardiac geometry index (wall thickness/diameter ratio) increases in BI 749327 group, depicting more concentric hypertrophy (*$P = 0.02$, ANCOVA).

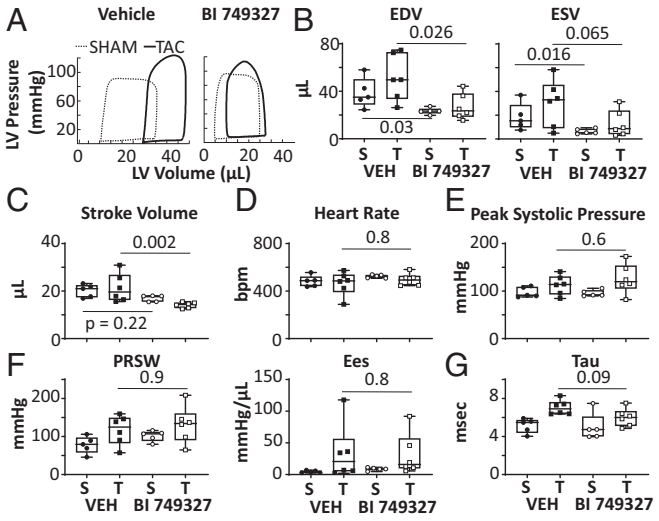

Fig. 4. In vivo pressure-volume analysis shows BI 749327 reduces preload but does not alter contractility. (*A*) Representative steady-state PV loops in both vehicle- and drug-treated groups. TAC increases LV volumes (right shift of the loop) with vehicle but less with BI 749327 treatment. (*B*–*G*) End-diastolic and end-systolic volume (EDV and ESV), stroke volume, heart rate, peak systolic pressure, LV contractility assessed by PRSW and Ees, and isovolumic relaxation assessed by time constant (tau). S, sham surgery; T, TAC; Veh, vehicle treatment; *P* values: Mann–Whitney *t* test between vehicle and drug treatment within sham or TAC groups (n = 5–6 per group).

growth factor-beta1 (*Tgfb1*), and tissue inhibitor of metalloproteinase 2 (*Timp2*). BI 749327 treatment suppressed expression of these genes (Fig. 5*B*), resulting in ∼40% decline in interstitial fibrosis determined from myocardial histopathology (Fig. 5*C*).

BI 749327 Reduces Renal Fibrosis Caused by UUO. To test the impact of BI 749327 in a model of renal fibrosis, we subjected mice to UUO, initiating BI 749327 or vehicle treament just before the intervention. UUO enhanced interstitial collagen deposition detected by picrosirius red staining, and this declined with BI 749327 in a dose-dependent manner (Fig. 6*A*). As TRPC6 is thought to activate myofibroblasts (18), tissue was stained for smooth muscle α-actin (αSMA) (Fig. 6*B*) and S100A4 (*SI Appendix*, Fig. S7*C*) and both declined with BI 749327 treatment. The fall in renal αSMA content with BI 749327 was dose dependent (Fig. 6*B* and *SI Appendix*, Fig. S8), with an IC_{50} of 306 nM. Gene expression for *Tgfb1* (Fig. 6*C*), collagen 4a1 (*Col4a1*), and fibronectin (*Fn1*) all declined with drug treatment (*SI Appendix*, Fig. S7 *A* and *B*). These changes were consistent with those in the TAC model. Reduced collagen I and IV protein levels with BI 749327 were confirmed by immunohistochemistry (*SI Appendix*, Fig. S7 *D* and *E*). BI 749327 also suppressed renal inflammatory cell infiltration, as reflected by reduced staining of the T cell marker CD3 (Fig. 6*D*), and reduced interstitial lesions (Fig. 6*E*). A macrophage marker (F4/80) did not meet statistical significance (*SI Appendix*, Fig. S7*F*, $P = 0.11$). Renal *Trpc6* rose fivefold in the UUO model, but unlike myocytes or heart, this did not decline with BI 749327 (*SI Appendix*, Fig. S9), and TRPC3 expression was undetectable in the kidney for all groups.

Discussion

This study reports the potent, selective TRPC6 antagonist (BI 749327) with pharmacokinetic properties compatible with oral dosing. Consistent with a proposed role for TRPC6 in controlling myofibroblast activation and fibrosis, BI 749327 suppressed interstitial fibrosis and associated molecular signaling in disease models of both the heart and kidney. While we did not determine if these changes reflected primarily prevention of de novo versus reversal of existing fibrosis, we and others have shown 1 wk of TAC generates fibrosis (35). Therefore, our

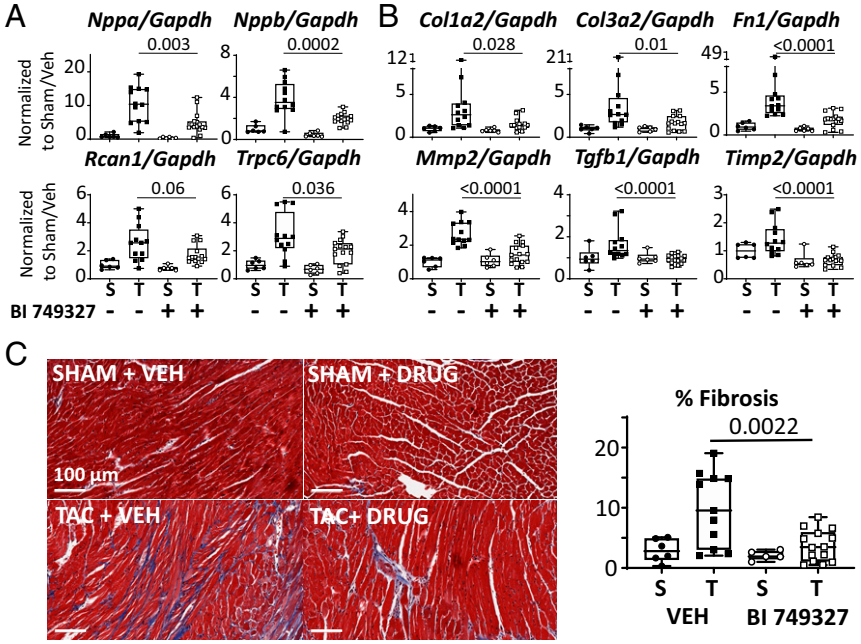

Fig. 5. BI 749327 reduces hypertrophic and profibrotic gene expression and myocardial fibrosis. (*A*) mRNA for hypertrophic marker genes are up-regulated in vehicle-treated TAC and reduced by BI 749327. S, sham; T, TAC. Sham data are not significantly different between groups. (*B*) mRNA for fibrosis-related genes in same myocardium. Elevation with TAC was suppressed by active drug therapy. (*C*, *Left*) Representative myocardial histology image at 20× magnification shows increased interstitial fibrosis in TAC-VEH that is suppressed by drug treatment. (*C*, *Right*) Summary data (*$P < 0.0001$; otherwise, *P* value noted on graph. Mann–Whitney test in drug treatment groups, no differences were present between shams. n = 6 per sham group, n = 12 TAC-VEH group, n = 15 TAC-BI 749327 group).

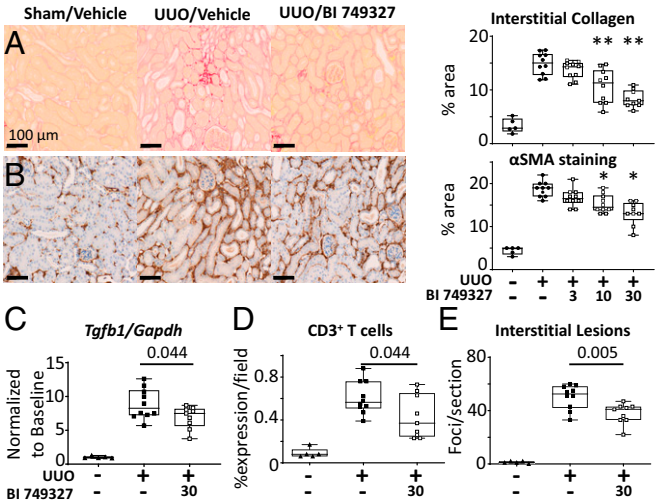

Fig. 6. BI 749327 treatment inhibits renal injury of mice after UUO. (*A*) Representative images of picrosirius red staining for interstitial collagen. BI 749327 treatment at 3, 10, and 30 mg/kg/d reduced collagen levels at the mid and high dose. (*B*) Representative images of αSMA immunohistochemical staining of kidney (**$P < 0.0005$, *$P < 0.01$ vs. UUO no treatment, one-way ANOVA with Dunnett's pairwise postcomparisons test). (*C–E*) BI 749327 treatment reduced UUO-induced (*C*) *Tgfb1* gene expression, (*D*) $CD3^+$ T cell expression, and (*E*) number of interstitial lesions (two-tailed unpaired *t* test).

results have the potential to reflect both. In the pressure-overloaded heart, BI 749327 also suppressed molecular markers of pathological hypertrophy, though interestingly this did not translate to reduced wall thickness or mass. However, chronic BI 749327 treatment also lowered left ventricular end-systolic and -diastolic volumes without altering contractility or systemic vascular resistance. This was observed with or without pressure overload. The volume changes, and not contractility or arterial vasodilation, likely explain a modest rise in fractional shortening. This finding suggests inhibition of TRPC6 by BI 749327 also has systemic effects on venous tone and/or circulatory volume. If translated to humans, such effects would be attractive for patients with heart failure and central vascular congestion. Unlike prior studies employing *Trpc6* gene deletion or expression of a dominant negative TRPC6 channel, the present data inhibit TRPC6 in adult animals after generating disease in vivo. Given the multiorgan role of TRPC6 in various diseases, the compound class deserves further development of its translational potential.

Prior attempts to develop TRPC6 antagonists have faced hurdles, with agents lacking sufficient selectivity and/or having poor pharmacokinetic profiles. Selectivity concerns are particularly relevant for the two closely related channels TRPC3 and TRPC7, and in this regard, BI 749327 is the most selective antagonist yet reported. The binding site for BI 749327 on TRPC6 remains unknown. Consequently structural features of the compound, and its protein interactions that impart selectivity, remain to be determined. The recently disclosed cryoelectron microscopy structure of TRPC6 (36) may ultimately help in this regard. Evidence for target engagement was provided by NFAT suppression in HEK293 cells, and a decline in *Trpc6* and *Rcan1* mRNA in myocytes and the heart, consistent with suppression of a positive NFAT–TRPC6 feedback loop (9). By contrast, we did not observe reduced *Trpc6* expression in the renal cortex of UUO mice. This may reflect alternative NFAT activation pathways in the kidney that maintain *Trpc6* gene expression despite BI 749327 efficacy in reducing associated profibrotic signaling genes and fibrosis, as in the myocardium. Renal cortical tissue may also provide more heterogeneous cell populations than in the heart, diluting mRNA changes relevant to particular cell types (e.g., podocytes and fibroblasts) with that of others. Overall, the data support BI 749327 engagement of its intended target.

The availability of a potent, selective TRPC6 antagonist suitable for in vivo pharmacology testing addresses an unmet need in defining the potential therapeutic opportunities from modulating this pathway. One limitation of prior genetic loss-of-function approaches is the potential to induce developmental adaptations. For example, the first *Trpc6* KO model exhibited hypertension coupled to up-regulation of *Trpc3* (37). Other models have shown minimal blood pressure changes (38), consistent with the lack of BI 749327 effects on blood pressure or heart rate. Another limitation of genetic models is that they may influence the composition of heterotetrameric channels that normally form between TRPC3, TRPC6, and TRPC7 subunits (39). The absence or overabundance of TRPC6 could alter the stoichiometry of remaining channel subunits, potentially generating compensatory functional channels. This is relevant, as we previously found that genetic deletion of neither TRPC3 nor TRPC6 alone ameliorated TAC-induced cardiac disease or fetal gene reexpression, whereas a double TRPC3/6 knockout was effective (3). In contrast, a dominant negative TRPC6 mouse model conferred modest protection (11). While we do not know if BI 749327 binding of TRPC6 cross-inhibits activity of other components in a TRPC6-based tetramer, the efficacy of BI 749327 in the current study suggests this is possible.

To our knowledge, no prior study has reported chronic TRPC6 inhibition reduces cardiac volumes (both end-diastolic and end-systolic volume), though this has also not been previously testable. TRPC6 contributes to acute contractility rise in hearts or cardiac muscle confronting an increase in afterload (40), and this could reduce chamber volumes in the intact heart. However, contractility was unaltered by BI 749327 in the current experiment despite sustained afterload elevation from TAC. The volume changes are also unlikely due to less fibrosis, as this would generally facilitate filling to increase not lower volumes, and similar preload decline was seen in sham mice that lack fibrosis. Rather, we believe volume decline likely reflects systemic effects of TRPC6 inhibition, lowering venous tone and/or circulating blood volume. The latter may involve the kidney, but this remains to be determined. TRPC6 is ubiquitously expressed in the vasculature and plays a key role in the vascular-tone response to α-adrenergic stimuli, vasopressin, angiotensin receptor stimulation, and arterial mechanical loading (24, 41). TRPC6 is also highly expressed in portal veins in mouse and rabbit where it regulates sympathetic-stimulated vascular tone (24). Regardless of the exact cause, lower preload from BI 749327 in chronic heart disease might contribute to reduced fibrosis by lowering wall stress and blunt central vascular congestion common to heart failure.

Our study has some limitations. First, evidence of target engagement by BI 749327 remains indirect, leveraging biomarkers engaged by the pathway. For the kidney, proof may require further cell-specific gene expression analysis. We did not test each disease model in TRPC6 KO mice to assess selectivity, as these models themselves alter the disease condition: TRPC6 gene deletion occurs before disease and up-regulation of other channels may compensate. The TAC cardiac model could not test if TRPC6 antagonism reverses lung congestion, a potential consequence of preload decline, as it modeled partially compensated hypertrophy and not heart failure. The UUO model generates interstitial fibrosis but not glomerular disease or proteinuria. Future studies in models that engage these abnormalities, such as diabetic nephropathy and other renal diseases, will be needed to test the therapeutic potential of BI 749327 for these conditions. Mice expressing gain-of-function TRPC6 mutations causing severe renal damage in humans rarely develop much disease (19), so such testing may ultimately be best done in humans.

In summary, we reveal in vivo evidence of therapeutic efficacy of an orally bioavailable TRPC6 antagonist to counter chronic profibrotic disease conditions. In addition to cardiac and renal disease, TRPC6 hyperstimulation is linked to important pathophysiology in the lung and in other tissues, and the favorable oral profile of BI 749327 supports exploration of its therapeutic role in these organs as well.

Materials and Methods

For detailed materials and methods, please refer to *SI Appendix*.

Electrophysiology. HEK293 cells transfected with mouse and human TRPC channels were voltage clamped using an EPC10 (HEKA), Axopatch 200B, or Axon Multiclamp 700B (Molecular Devices). Currents were acquired at 10 kHz and filtered at 2 or 2.9 kHz. The standard voltage ramp protocol was applied with a 4- to 5-s interval and comprised an 80-ms step at −80 mV, a 320-ms ramp to +80 mV, and a 40-ms voltage step at +80 mV.

In Vitro Cellular Assays. Neonatal rat ventricular myocytes were isolated from newborn Sprague-Dawley rat pups and stimulated with angiotensin II followed by vehicle or BI 749327 treatment. HEK293T cells were cultured to 70% confluence, transfected with plasmids expressing a NFAT luciferase reporter and another expressing WT-TRPC6, gain-of-function TRPC6 mutants (P112Q, M132T, R175Q, R895C, and R895L), or empty vector pcDNA3.1. Renilla-luciferase plasmid was transfected as an internal control.

Pharmacokinetic Studies. Pharmacokinetics of BI 749327 were investigated in male CD-1 mice (Janvier) at dose levels of 3, 10, and 30 mg/kg and at 30 mg/kg in B6129F1 mice (Taconic Biosciences). Serial blood sampling was performed via puncture of the saphenous vein and samples were collected using EDTA-coated microtainers (Microvette).

In Vivo Pressure-Overload Model. Mice received daily gavage with methylcellulose/Tween-80 vehicle starting 1 wk before TAC surgery. After 1 wk post-TAC, mice were orally gavaged with daily vehicle or BI 749327 treatment. Cardiac function was assessed by serial echocardiography (Acuson Sequoia and VisualSonic Vevo) followed by terminal pressure-volume analysis (PowerLab, AD Instruments) after 8 wk post-TAC.

In Vivo Unilateral Ureteral Obstruction Model. A midline laparotomy was performed and the left ureter was isolated and ligated at the boundary of the lower renal pole to induce irreversible UUO.

Statistical Analysis. For multiple comparisons, ordinary one-way ANOVA with Holm–Sidak posttest or Dunnett's posttest was used for parametric tests (GraphPad Prism 7.0) and Welch's ANOVA with Games–Howell posttest for nonparametric tests (Minitab 18), as appropriate. Time course data were analyzed using a covariance design (SYSTAT 10.2 and Minitab 18). For single comparisons, unpaired *t* test or a Mann–Whitney nonparametric test were used. Data were plotted as mean ± SEM with a P value ≤ 0.05 considered statistically significant.

ACKNOWLEDGMENTS. We acknowledge the contributions of Glenn Gibson, Kathleen Lincoln, and Valentina Berger toward the in vivo renal pharmacology studies. This work was supported by Boehringer Ingelheim and NIH Grants R01-HL-119012, HL-131358, R35-HL135827, and PO-HL107153 (to D.A.K.), T32 Grant T32-HL-7227 (to B.L.L.), and American Heart Association Postdoctoral Fellowship Grants 18CDA34110140 (to M.J.R.) and 18POST33960157 (to G.K.M.).

1. Dietrich A, Gudermann T (2014) TRPC6: Physiological function and pathophysiological relevance. *Handb Exp Pharmacol* 222:157–188.
2. Hofmann K, et al. (2017) Classical transient receptor potential 6 (TRPC6) channels support myofibroblast differentiation and development of experimental pulmonary fibrosis. *Biochim Biophys Acta Mol Basis Dis* 1863:560–568.
3. Seo K, et al. (2014) Combined TRPC3 and TRPC6 blockade by selective small-molecule or genetic deletion inhibits pathological cardiac hypertrophy. *Proc Natl Acad Sci USA* 111: 1551–1556.
4. Reiser J, et al. (2005) TRPC6 is a glomerular slit diaphragm-associated channel required for normal renal function. *Nat Genet* 37:739–744.
5. Winn MP, et al. (2005) A mutation in the TRPC6 cation channel causes familial focal segmental glomerulosclerosis. *Science* 308:1801–1804.
6. Hofstra JM, et al. (2013) New TRPC6 gain-of-function mutation in a non-consanguineous Dutch family with late-onset focal segmental glomerulosclerosis. *Nephrol Dial Transplant* 28:1830–1838.
7. Heeringa SF, et al. (2009) A novel TRPC6 mutation that causes childhood FSGS. *PLoS One* 4:e7771.
8. Gigante M, et al. (2011) TRPC6 mutations in children with steroid-resistant nephrotic syndrome and atypical phenotype. *Clin J Am Soc Nephrol* 6:1626–1634.
9. Kuwahara K, et al. (2006) TRPC6 fulfills a calcineurin signaling circuit during pathologic cardiac remodeling. *J Clin Invest* 116:3114–3126.
10. Xie J, et al. (2012) Cardioprotection by Klotho through downregulation of TRPC6 channels in the mouse heart. *Nat Commun* 3:1238.
11. Wu X, Eder P, Chang B, Molkentin JD (2010) TRPC channels are necessary mediators of pathologic cardiac hypertrophy. *Proc Natl Acad Sci USA* 107:7000–7005.
12. Fuchs B, et al. (2011) Diacylglycerol regulates acute hypoxic pulmonary vasoconstriction via TRPC6. *Respir Res* 12:20.
13. Weissmann N, et al. (2012) Activation of TRPC6 channels is essential for lung ischaemia-reperfusion induced oedema in mice. *Nat Commun* 3:649.
14. Makarewich CA, et al. (2014) Transient receptor potential channels contribute to pathological structural and functional remodeling after myocardial infarction. *Circ Res* 115:567–580.
15. Koitabashi N, et al. (2010) Cyclic GMP/PKG-dependent inhibition of TRPC6 channel activity and expression negatively regulates cardiomyocyte NFAT activation Novel mechanism of cardiac stress modulation by PDE5 inhibition. *J Mol Cell Cardiol* 48:713–724.
16. Chung HS, et al. (2017) Transient receptor potential channel 6 regulates abnormal cardiac S-nitrosylation in Duchenne muscular dystrophy. *Proc Natl Acad Sci USA* 114: E10763–E10771.
17. Wang L, et al. (2015) Gq signaling causes glomerular injury by activating TRPC6. *J Clin Invest* 125:1913–1926.
18. Davis J, Burr AR, Davis GF, Birnbaumer L, Molkentin JD (2012) A TRPC6-dependent pathway for myofibroblast transdifferentiation and wound healing in vivo. *Dev Cell* 23:705–715.
19. Krall P, et al. (2010) Podocyte-specific overexpression of wild type or mutant trpc6 in mice is sufficient to cause glomerular disease. *PLoS One* 5:e12859.
20. Wu YL, et al. (2017) Inhibition of TRPC6 channels ameliorates renal fibrosis and contributes to renal protection by soluble klotho. *Kidney Int* 91:830–841.
21. Weissmann N, et al. (2006) Classical transient receptor potential channel 6 (TRPC6) is essential for hypoxic pulmonary vasoconstriction and alveolar gas exchange. *Proc Natl Acad Sci USA* 103:19093–19098.
22. He LP, Hewavitharana T, Soboloff J, Spassova MA, Gill DL (2005) A functional link between store-operated and TRPC channels revealed by the 3,5-bis(trifluoromethyl) pyrazole derivative, BTP2. *J Biol Chem* 280:10997–11006.
23. Merritt JE, et al. (1990) SK&F 96365, a novel inhibitor of receptor-mediated calcium entry. *Biochem J* 271:515–522.
24. Inoue R, et al. (2001) The transient receptor potential protein homologue TRP6 is the essential component of vascular alpha(1)-adrenoceptor-activated Ca(2+)-permeable cation channel. *Circ Res* 88:325–332.
25. Urban N, et al. (2016) Identification and validation of larixyl acetate as a potent TRPC6 inhibitor. *Mol Pharmacol* 89:197–213.
26. Hafner S, et al. (2018) A (+)-larixol congener with high affinity and subtype selectivity toward TRPC6. *ChemMedChem* 13:1028–1035.
27. Miehe S, et al. (2012) Inhibition of diacylglycerol-sensitive TRPC channels by synthetic and natural steroids. *PLoS One* 7:e35393.
28. Urban N, Hill K, Wang L, Kuebler WM, Schaefer M (2012) Novel pharmacological TRPC inhibitors block hypoxia-induced vasoconstriction. *Cell Calcium* 51:194–206.
29. Spassova MA, Hewavitharana T, Xu W, Soboloff J, Gill DL (2006) A common mechanism underlies stretch activation and receptor activation of TRPC6 channels. *Proc Natl Acad Sci USA* 103:16586–16591.
30. Ding M, et al. (2018) Pyrazolo[1,5-a]pyrimidine TRPC6 antagonists for the treatment of gastric cancer. *Cancer Lett* 432:47–55.
31. Maier T, et al. (2015) Discovery and pharmacological characterization of a novel potent inhibitor of diacylglycerol-sensitive TRPC cation channels. *Br J Pharmacol* 172: 3650–3660.
32. Motoyama K, et al. (2018) Discovery of a bicyclo[4.3.0]nonane derivative DS88790512 as a potent, selective, and orally bioavailable blocker of transient receptor potential canonical 6 (TRPC6). *Bioorg Med Chem Lett* 28:2222–2227.
33. Schaldecker T, et al. (2013) Inhibition of the TRPC5 ion channel protects the kidney filter. *J Clin Invest* 123:5298–5309.
34. Onohara N, et al. (2006) TRPC3 and TRPC6 are essential for angiotensin II-induced cardiac hypertrophy. *EMBO J* 25:5305–5316.
35. Takimoto E, et al. (2005) Chronic inhibition of cyclic GMP phosphodiesterase 5A prevents and reverses cardiac hypertrophy. *Nat Med* 11:214–222.
36. Tang Q, et al. (2018) Structure of the receptor-activated human TRPC6 and TRPC3 ion channels. *Cell Res* 28:746–755.
37. Dietrich A, et al. (2005) Increased vascular smooth muscle contractility in TRPC6-/- mice. *Mol Cell Biol* 25:6980–6989.
38. Eckel J, et al. (2011) TRPC6 enhances angiotensin II-induced albuminuria. *J Am Soc Nephrol* 22:526–535.
39. Hofmann T, Schaefer M, Schultz G, Gudermann T (2002) Subunit composition of mammalian transient receptor potential channels in living cells. *Proc Natl Acad Sci USA* 99:7461–7466.
40. Seo K, et al. (2014) Hyperactive adverse mechanical stress responses in dystrophic heart are coupled to transient receptor potential canonical 6 and blocked by cGMP-protein kinase G modulation. *Circ Res* 114:823–832.
41. Hill-Eubanks DC, Gonzales AL, Sonkusare SK, Nelson MT (2014) Vascular TRP channels: Performing under pressure and going with the flow. *Physiology (Bethesda)* 29: 343–360.